A topological classification of convex bodies

Gábor Domokos · Zsolt Lángi · Tímea Szabó

Abstract The shape of homogeneous, generic, smooth convex bodies as described by the Euclidean distance with nondegenerate critical points, measured from the center of gravity represents a rather restricted class $\mathcal{M}_C$ of Morse-Smale functions on $\mathbb{S}^2$. Here we show that even $\mathcal{M}_C$ exhibits the complexity known for general Morse-Smale functions on $\mathbb{S}^2$ by exhausting all combinatorial possibilities: every 2-colored quadrangulation of the sphere is isomorphic to a suitably represented Morse-Smale complex associated with a function in $\mathcal{M}_C$ (and vice versa). We prove our claim by an inductive algorithm, starting from the path graph P_2 and generating convex bodies corresponding to quadrangulations with increasing number of vertices by performing each combinatorially possible vertex splitting by a convexity-preserving local manipulation of the surface. Since convex bodies carrying Morse-Smale complexes isomorphic to P_2 exist, this algorithm not only proves our claim but also generalizes the known classification scheme in [36]. Our expansion algorithm is essentially the dual procedure to the algorithm presented by Edelsbrunner et al. in [21], producing a hierarchy of increasingly coarse Morse-Smale complexes. We point out applications to pebble shapes.

Gábor Domokos
Dept. of Mechanics, Materials and Structures, Budapest University of Technology, Műegyetem rakpart 1-3., Budapest, Hungary, 1111
E-mail: domokos@iit.bme.hu

Zsolt Lángi
Dept. of Geometry, Budapest University of Technology, Egry József u. 1., Budapest, Hungary, 1111
E-mail: zlangi@math.bme.hu

Tímea Szabó
Dept. of Mechanics, Materials and Structures, Budapest University of Technology, Műegyetem rakpart 1-3., Budapest, Hungary, 1111
E-mail: tszabo@szt.bme.hu

1 Introduction

The study of static equilibria of convex bodies was initiated by Archimedes [27] and attracts even current interest (cf. [12], [13], [14], [28] or [37]). In mathematical terms, a convex body $K \in \mathcal{K}$ can be characterized by the scalar distance function $r_K : \mathbb{S}^2 \to (0, \infty)$, measured from the center of mass of K. Static equilibrium points coincide with critical points of r_K, characterized by $\nabla r_K = 0$. We call K *generic* if r_K is a Morse-Smale function, i.e. it has only non-degenerate critical points and the stable and unstable manifolds of any two critical points (under the flow induced by ∇r_K) are transverse [38]. If we denote the numbers of stable, unstable and saddle-type critical points by S, U, H, respectively, then $\{S, U\}$ is called the *primary equilibrium class* of K and the number of saddles can be obtained via the Poincaré-Hopf formula as

$$H = S + U - 2. \tag{1}$$

In [36], the above classification was introduced and it was shown that the primary classification system is complete in the sense that there are no empty primary classes. Our current motivation is to go beyond this result and establish the completeness according to a more refined (secondary) classification for generic convex bodies, based on the topological arrangement of equilibria, i.e., to show that every combinatorially possible arrangement physically also exists.

If K is generic then the *Morse-Smale complex* of r_K consists of the intersections of the stable and unstable manifolds of each of the critical points and it is a CW complex of dimension 1 on $\mathbb{S}^2$, i.e it is a graph embedded in $\mathbb{S}^2$. One possible representation of this graph is a special, 3-colored quadrangulation $Q^{3\star}(K)$ on $\mathbb{S}^2$ and we refer to it as the *primal representation* of the Morse-Smale complex. The vertices of $Q^{3\star}(K)$ correspond to the critical points and they can be colored according to the stability-type by S, U, H, respectively. According to [21], $Q^{3\star}(K)$ is a special quadrangulation where the colors of the vertices on every quadrangle run in cyclic order S, H, U, H and the numbers of colored vertices satisfy Eq.(1). We denote the set of such 3-colored quadrangulations by $\mathcal{Q}^{3\star}$ and we call $Q^{3\star}(K) \in \mathcal{Q}^{3\star}$ the *secondary equilibrium class* of K. Figure 1 illustrates two convex bodies, their associated gradient fields, their Morse-Smale complexes and their secondary classes.

Our main goal is to prove that the secondary classification is, similarly to the primary one, complete, i.e. that

Theorem 1 *For every 3-colored quadrangulation $Q^{3\star} \in \mathcal{Q}^{3\star}$ of $\mathbb{S}^2$, there is a homogeneous convex body K, with a C^∞-class boundary, such that r_K is Morse-Smale, and the Morse-Smale complex of r_K is isomorphic to $Q^{3\star}$ via an embedding preserving isomorphism.*

In order to explain the main idea of our proof we have to introduce an alternative, equivalent graph representation of the Morse-Smale complex. By adding the $S - U$ diagonal edges to all $Q^{3\star} \in \mathcal{Q}^{3\star}$ and removing all H-colored vertices we introduce the *quasi-dual* representation [20] and we obtain the set $\mathcal{Q}^2$ of two-colored quadrangulations on $\mathbb{S}^2$ (cf. Figure 2). We denote the two-colored quadrangulation associated with the convex body K by $Q^2(K)$. We also introduce $\mathcal{Q}^2_n \subset \mathcal{Q}^2$ for the 2-colored (S, U) quadrangulations of the sphere with exactly $S + U = n$
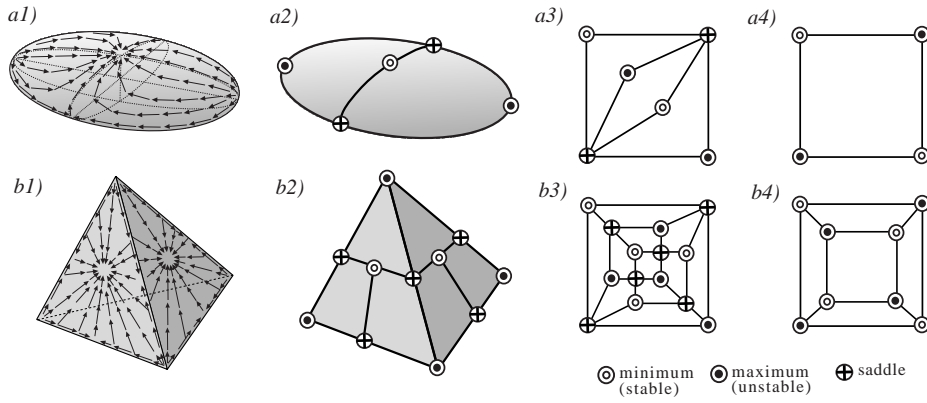
Fig. 1 Examples for equilibrium classes. a1) Gradient field of tri-axial ellipsoid in primary class $\{2, 2\}$. a2) Morse-Smale complex associated with the tri-axial ellipsoid. a3) planar drawing of the graph representing the secondary class of the tri-axial ellipsoid. a4) quasi-dual representation of the complex. b1) Gradient field of tetrahedron in primary class $\{4, 4\}$. b2) Morse-Smale complex associated with the tetrahedron. b3) planar drawing of the graph representing the secondary class of the tetrahedron. b4) quasi-dual representation of the complex

vertices and the class of convex bodies with exactly $S + U = n$ extremal points will be denoted by $\mathcal{K}_n \subset \mathcal{K}$. It is relatively easy to see (as we show in Section 2 based on results from [5], [10] and [32]) that by subsequent applications of an operation called *face contraction* (where two diagonal vertices in a quadrangular face are merged and the resulting double edges are also merged) an arbitrarily selected two-colored quadrangulation $\bar{Q}^2 \in \mathcal{Q}_n^2$ can be collapsed onto the path graph P_2 (the unique graph with 2 vertices and one edge [25]) via a sequence of $(n-1)$ graphs. If we list the latter in reverse order, we obtain what we call *combinatorial expansion sequences:*

$$Q_2^2 \equiv P_2, Q_3^2, Q_4^2, \dots, Q_{n-1}^2, Q_n^2 \equiv \bar{Q}^2 \text{ such that } Q_i^2 \in \mathcal{Q}_i^2. \qquad (2)$$

Subsequent elements of (2) are connected via *vertex splittings* (cf.[5], [10]), the inverse operation of face contraction. Both face contraction and vertex splitting can be carried out on any $Q^2 \in \mathcal{Q}_n^2, n > 2$, and thus the sequences (2) can be generated both forward (vertex splittings) and backward (face contractions). Neither the forward nor the backward sequence is unique. To prove Theorem 1, in Section 3 we show that each combinatorially possible vertex splitting can be realized on convex bodies by a convexity-preserving, local manipulation of the surface (consisting of two consecutive, local truncations) which we call *equilibrium splitting* . By this operation we can create *geometric expansion sequences*

$$K_2, K_3, K_4, \dots, K_{n-1}, K_n \equiv \bar{K} \text{ such that } K_i \in \mathcal{K}_i, \qquad (3)$$

which are generated in such a way that they are linked to an arbitrarily, a priori given combinatorial expansion sequence (2) via

$$Q^2(K_i) = Q_i^2. \qquad (4)$$

We remark that a similar strategy of determining a sequence of geometric transformations appears also in the proof of Andreev's theorem [1], [34]. Combinatorial

sequences belonging to an arbitrary graph $\bar{Q}^2 \in \mathcal{Q}_n^2$ can be generated by running (2) in reverse order, arriving at P_2. Since convex bodies in class $\mathcal{K}_2$ carrying Morse-Smale complexes homeomorphic to P_2 exist (cf. [36]), subsequently we can run (3) forward to obtain the desired convex body $\bar{K}$ with $Q^2(\bar{K}) = \bar{Q}^2$. This algorithm not only proves Theorem 1 but also generalizes the primary scheme of [36], which uses only the numbers S, U of stable and unstable equilibria to classify convex shapes. We remark that an essential part of this generalization is the geometric truncation algorithm described in Section 3 since, as it was shown in [30], combinatorial expansion sequences based on the the geometric truncations presented in [36] are *not* capable of generating all secondary equilibrium classes. We also remark that, unlike combinatorial sequences (2), which can be run both forward and backward, our geometrical expansion sequences (3) can be run only forward from an arbitrary initial convex body K. Nevertheless, in a different setting, the geometric analogy of face contraction was considered in [9].

The local truncations associated with each geometric expansion step are extremely delicate. To have the ability of performing *any* combinatorially possible splitting (i.e. to obtain a convex body with the desired Morse-Smale complex) one has to render the vicinity of the given critical point *arbitrarily sensitive* before the actual splitting is achieved with a planar truncation. We achieve arbitrary sensitivity in Lemma 9 by constructing a preliminary truncation with a sphere the radius of which is sufficiently close to the distance of the equilibrium point to be split from the centre of gravity. If only the critical point is specified, however, the combinatorial structure of the splitting is arbitrary then the geometric task is substantially simpler [36].

Our expansion algorithm is essentially the dual procedure to the one presented by Edelsbrunner et al. [21] (cf. also [15]), producing a hierarchy of increasingly coarse Morse-Smale complexes (i.e. running combinatorial expansion sequences in reverse order compared to (2)); a topic attracting current interest in computational topology (cf. [6] or [26]). Beyond illustrating that the secondary classification scheme for generic convex bodies is complete (i.e. the Morse-Smale complexes of generic convex bodies exhausts all possible combinatorial possibilities) and offering a modest link between Morse theory and convex geometry, geometric expansion sequences defined in equation (3) appear to be the natural building blocks for the mathematical description of pebble shape evolution under collisional abrasion.

Our paper is structured as follows. In Section 2 we introduce our combinatorial tools and show how Theorem 1 follows from the main geometric lemma: Lemma 3. In Section 3, we prove Lemma 3 in three steps, formulated in Lemmas 4, 5 and 6, and proved in Subsections 3.1, 3.2 and 3.3, respectively, by means of other auxiliary lemmas. We illustrate our results and discuss some related issues (including pebble abrasion) in Section 4.

2 Preliminaries and the proof of Theorem 1

In this section, first, we introduce the background for the proof, and, finally, show how Theorem 1 follows from our main lemma: Lemma 3. Throughout this section, by the *center* of a convex body K we mean its center of gravity. Furthermore,
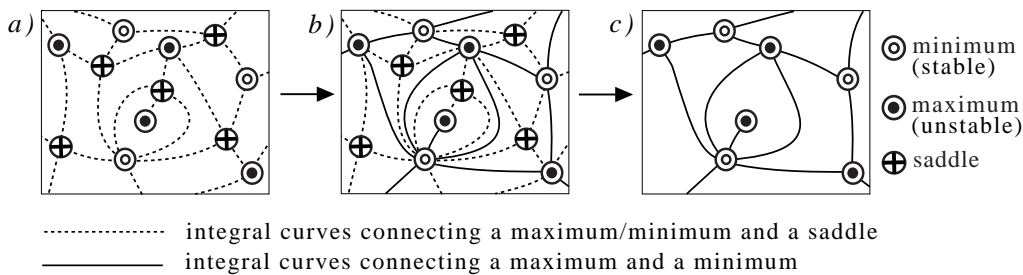
the *Morse-Smale complex of K* is meant to be the Morse-Smale complex defined on bd K by the Euclidean distance function from the center of K. If we measure distance from a different point w, then we write about the *Morse-Smale complex of K with respect to w*.

Let us recall that a *quadrangulation* of $\mathbb{S}^2$ is the embedding of a finite graph on the 2-sphere such that it may have multiple edges and each face is bounded by a closed walk of length 4 (cf. [2] or [10]). We note that this closed walk is permitted to contain the same vertex or edge more than once, and, following Archdeacon et al. [2], we regard the path graphs (cf. [25]) P_2 and P_3, the only trees with 2 or 3 vertices, respectively, as quadrangulations. Let $\mathcal{Q}^0$ and $\mathcal{Q}$ denote the class of not-colored, and 2-colored quadrangulations, respectively. Observe that every quadrangulation is bipartite, and thus, 2-colorable, and that any quadrangulation (connected bipartite graph) can be colored in a unique way. Furthermore, let $\mathcal{Q}^{3\star}$ be the class of 3-colored quadrangulations, with colors (S, U, H), satisfying $S + U - H = 2$ (cf. 1), and $deg(v) = 4$ for any $v \in H$.

An important tool in describing Morse-Smale complexes of $\mathbb{S}^2$ is the so-called Quadrangle Lemma from [21].

Lemma 1 (Edelsbrunner et al.) *Each region of the Morse complex is a quadrangle with maximum, saddle, minimum, and saddle point as vertices, in this order around the region. The boundary is possibly glued to itself along edges or vertices.*

Based on this lemma, a complete combinatorial description of a Morse-Smale complex can be given ([21], [20] and [38]): it corresponds to a 3-colored quadrangulation in $\mathcal{Q}^{3\star}$, where colors correspond to the 3 types of non-degenerate critical points (maxima, minima and saddles), satisfies the Quadrangle Lemma, and the degree of every saddle is 4. We follow Dong et al. [20] and call this representation of the complex the *primal* Morse-Smale graph. Saddle points can be removed from the primal Morse-Smale graph without losing information: first we connect maxima and minima in the quadrangles, then cancel saddle points and edges incident to them (see Figure 2). We call this representation the *quasi-dual* Morse-Smale graph (cf. [20]).

> $\cdots\cdots\cdots$ integral curves connecting a maximum/minimum and a saddle
> ————— integral curves connecting a maximum and a minimum

Fig. 2 Different representations of a Morse-Smale complex. a) Primal Morse-Smale graph in class $\mathcal{Q}^{3\star}$ b) Primal Morse-Smale graph with the maxima and minima connected c) Quasi-dual Morse-Smale graph in class $\mathcal{Q}$

The following lemma is a slight generalization of results of Bagatelj [5], and also Negami and Nakamoto [32]. To state it, for any quadrangulation $Q \in \mathcal{Q}^0$ and

face F of Q with boundary walk $v_1e_1v_2e_2v_3e_3v_4e_4v_5$, where $v_1 = v_5$ and edges are $e_i = \{v_i, v_{i+1}\}$, $i = 1, 2, 3, 4$ (cf. Figure 3 a), left), we define the *contraction of the face F* as the following: shrink the region F by identifying the vertices v_1 and v_3, the edges e_1 and e_2, and the edges e_3 and e_4. Note that this operation on Q is invertible; the inverse operation is called *vertex splitting*.

Lemma 2 *Any quadrangulation $Q \in \mathcal{Q}^0$ can be reduced to the path graph P_2 via a sequence of face contractions, or equivalently, Q can be obtained from P_2 via a sequence of vertex splittings.*

Proof Let $Q \in \mathcal{Q}^0$ and face F of Q with boundary walk $v_1e_1v_2e_2v_3e_3v_4e_4v_5$, where $v_1 = v_5$ and edges are $e_i = \{v_i, v_{i+1}\}$, $i = 1, 2, 3, 4$. If Q is not simple, these vertices and edges may not be distinct, however, the definition of quasi-dual representation (i.e. that these graphs have been generated by removing the saddle points of degree 4 from the triangular representation) admits only two kinds of coincidences: two diagonal vertices v_2 and v_4 may coincide, and in this case the edges e_2 and e_3 may coincide. These two cases are shown in Figure 3 b) and c), left. Note that in Figure 3 b) the internal domain bordered by the edges e_2 and e_3 is not a quadrangular face but necessarily contains additional vertices.

The proof is based on the observation, illustrated in Figure 3, that the contracted graph has one less vertex than Q, and is contained in the same class $\mathcal{Q}^0$. Since any graph with at least three vertices can be contracted, we may reduce Q to the only graph $P_2 \in \mathcal{Q}^0$ with two vertices.
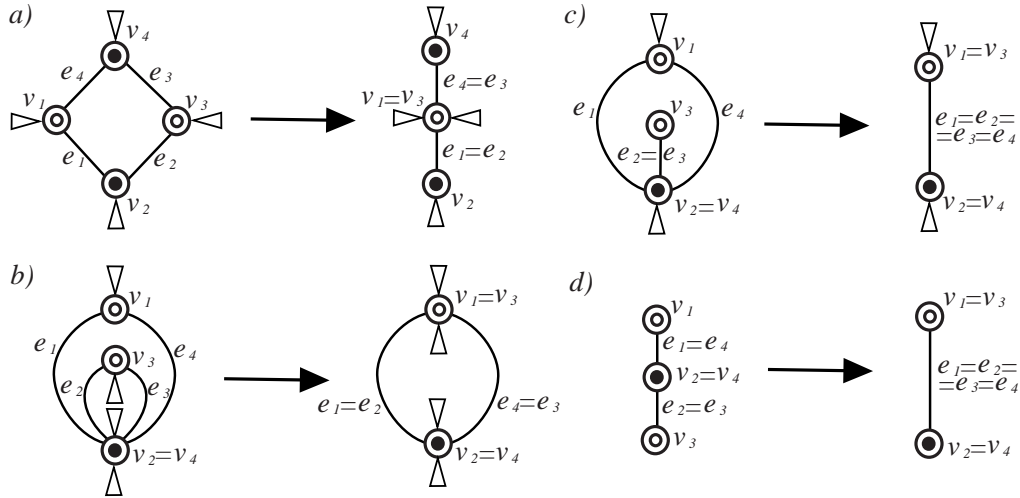
Fig. 3 Contraction of a face of a graph in class $\mathcal{Q}^2$. Like in [10], triangles incident to some vertices indicate that one or more edges *may* occur at that position around the vertex. Here, v_1 and v_3 are minimum points. The counterpart of the illustrated operation, which removes a maximum point from the graph, can be performed by switching the colors. a) Contraction of a generic face. b) Contraction of a face with a double vertex. c) Contraction of a face with a double edge. d) Contraction of the path graph P_3.

Remark 1 As any quadrangulation $Q \in \mathcal{Q}^0$ can be colored with 2 colors in a unique way, Lemma 2 can be applied for 2-colored quadrangulations, i.e. for quasi-dual representations of Morse-Smale complexes. This process can be extended to primal graph representations as well via the natural identification of the elements of $\mathcal{Q}^0$ and $\mathcal{Q}^{3\star}$.

Since a face contraction can be applied to any face of a quadrangulation, the sequence of graphs from Q to P_2 is, in general, not unique. In special applications additional criteria may be applied to single out one sequence among the combinatorially possible ones. Face contraction on multigraphs was already used in [21] and [15] to simplify Morse-Smale complexes. Edelsbrunner et al. used the primal representation of the complex in which a face contraction (defined in the quasi-dual representation) emerges as a double *edge contraction* [16]. Their goal was to produce a hierarchy of increasingly coarse Morse-Smale complexes, therefore they applied an extra metric criteria (growing height differences on the edges of the graph) which resulted in an unambiguous sequence of graphs. This algorithm was also used in [18] to identify macroscopically perceptible static equilibrium points of 3D scanned pebbles.

Definition 1 *If a convex body K, with C^∞-class boundary, satisfies the property that*

- *the Euclidean distance function of K is Morse-Smale;*
- $\operatorname{bd} K$ *has nonzero principal curvatures at any critical point of this function;*

then we say that K satisfies property (*).

Our main lemma is the following.

Lemma 3 *There is a convex body K_0 satisfying (*) with only one stable and only one unstable equilibrium point. Furthermore, if K is a convex body satisfying (*) with Morse-Smale graph Q, and Q' is obtained from Q via any vertex splitting, then there is a convex body K' satisfying (*), with Morse-Smale graph Q'.*

We prove Lemma 3 in Section 3.

Proof (Proof of Theorem 1) Let $Q \in \mathcal{Q}^{3\star}$ be given. Then, by Lemma 2 and Remark 1, there is a sequence $Q_1, Q_2 \ldots, Q_n \in \mathcal{Q}^{3\star}$ such that $Q_1 = P_2$, $Q_n = Q$ and for $i = 1, 2, \ldots, n-1$, Q_{i+1} is obtained from Q_i via a suitable vertex splitting. Since the only graph in $\mathcal{Q}^{3\star}$ with two vertices is P_2, Lemma 3 states that there is a convex body K_1, satisfying (*), with graph P_2. Thus applying Lemma 3 $(n-1)$ times, we obtain that for any $i = 2, 3, \ldots, n$ (in particular, for $i = n$) there is a convex body K_i satisfying (*) and having graph Q_i.

3 Proof of Lemma 3

The proof is based on three lemmas.

Lemma 4 (Smoothing subroutine) *If K is a convex body with C^1-class boundary such that its distance function is Morse-Smale, every equilibrium point of K has a C^2-class neighborhood, and its principal curvatures are positive at any such point, then there is a C^∞-class convex body K' satisfying (*) such that K and its Morse-Smale graph are arbitrarily small perturbations of K' and its Morse-Smale-graph. Furthermore, there is a C^∞-class convex body K satisfying (*) with only one stable and one unstable point.*

Lemma 5 (Spherical neighborhood) *Let K be a C^∞-class convex body satisfying (*) and let p be any stable or unstable point of K. Assume that the center of mass of K is the origin o. If p is stable, let $r > ||p||$, and if p is unstable, $0 < r < ||p||$ be arbitrary. Then there is a convex body K' satisfying (*) such that*

- *K' and its Morse-Smale graph are arbitrarily small perturbations of K and its Morse-Smale graph, respectively,*
- *the stable/unstable point p' of K associated to p has a spherical neighborhood in $\operatorname{bd} K'$ of radius r' arbitrarily close to r.*

Lemma 6 (Vertex splitting) *Let K be a C^∞-class convex body satisfying (*), with Morse-Smale graph $Q \in \mathcal{Q}^{3\star}$. Let p be a stable or unstable point of K, and Q' be a graph obtained from Q be splitting the vertex p in any given way. Assume that p has a spherical neighborhood in $\operatorname{bd} K$ with radius r' sufficiently close to some suitable chosen r with $r > ||p||$ if p is stable and $0 < r < ||p||$ if p is unstable. Then there is a C^∞-class convex body K' with Morse-Smale graph Q' satisfying (*).*

3.1 Proof of Lemma 4

Let o denote the center of mass of K, and observe that $o \in \operatorname{int} K$. Let f denote the *distance function* of K; that is, f is defined by $f(u) = \min\{\lambda : \lambda \geq 0, u \in \lambda K\}$ (cf. [7]). Let $h : \mathbb{R}^3 \to \mathbb{R}$ be a nonnegative, C^∞-class function such that $\operatorname{supp} h \subseteq \mathbf{B}$ and $\int_{\mathbb{R}^3} h(x) \, dx = 1$. Such a function is called by various names in the literature: *mollifier* (cf. [22]), or *bump function* (cf. [29]) or *probability distribution*. Clearly, we may choose h in a way that its symmetry group is O^3. Observe that by setting $h_t(x) = \frac{h(x/t)}{t^3}$, we obtain a family of C^∞-class functions with $\operatorname{supp} h_t \subseteq t\mathbf{B}$ and $\int_{\mathbb{R}^3} h_t(x) \, dx = 1$.

Let us define the function $g_t : \mathbb{R}^3 \to \mathbb{R}$ as the convolution

$$g_t(x) = \int_{\mathbb{R}^3} f(x-y) h_t(y) \, dy.$$

Clearly, for every t, g_t is C^∞-class, and as the integral average of convex functions is convex, it is convex. In particular, it follows that the set $K_t = g_t^{-1}([0,1])$ is compact and convex, and hence it is a convex body for sufficiently small values of t. Thus, applying the Implicit Function Theorem for k times continuously differentiable functions, it follows that $\operatorname{bd} K_t$ is a C^∞-class submanifold of $\mathbb{R}^n$.

Furthermore, it is known (cf. [24] or [29]), that if U is a compact set and f is C^n-class on U for some $2 \leq n < \infty$, then on U g_t converges uniformly to f,

together with its derivatives up to order n, as $t \to 0$. Thus, for sufficiently small values of t, that is, for any $t \in [0, \varepsilon]$ for some $\varepsilon > 0$, the Morse-Smale complex of K_t with respect to o is homeomorphic to that of K; and bd K_t has nonzero principal curvatures at the critical points of K. This implies that K_t satisfies (*).

We are left to show that, for small values of t, the Morse-Smale complex of K_t with respect to its center is homeomorphic to that with respect to o. To do this, we observe that for any $t \in [0, \varepsilon]$ there is some $\rho > 0$ such that the Morse-Smale complex of K_t with respect to u is homeomorphic to that with respect to o, for any $u \in \operatorname{int} \mathbf{B}_\rho$. Let the radius of the largest such ball be $\rho(t)$. Clearly, $\rho(t)$ is a continuous function of t, and thus, by compactness, there is a value of ρ such that for any $t \in [0, \varepsilon]$, the Morse-Smale complex of K_t with respect to any point of $\operatorname{int} \mathbf{B}_\rho$ is homeomorphic to that with respect to o. Note that the center o_t of K_t tends to o as $t \to 0$. Thus, if t is sufficiently small, $|o_t| < \rho$. Choosing t with this property and setting $K' = K_t$, the assertion readily follows.

To prove the second part, we apply our method for the mono-monostatic convex body K_0 constructed in [36]. This body is C^1-class at every boundary point, and, apart from the two equilibrium points, it is C^2-class. Furthermore, at the two equilibrium points the one-sided curvatures in every normal section are positive. Thus, applying our method yields the assertion.

Remark 2 Note that as the symmetry group of h is O^3, if $p \in \operatorname{bd} K$ has a spherical cap neighborhood, then so does the corresponding point of K'.

3.2 Proof of Lemma 5

Let o be the center of gravity of K, and assume that $p = (0, 0, 1)$. Then the condition that p is nondegenerate is equivalent to saying that $||p||\kappa_1 \neq 1 \neq ||p||\kappa_2$, where κ_1 and κ_2 are the two principal curvatures of bd K at p.

Now we define a two-parameter family of truncations of K, denoted by $K_R(\varepsilon)$. Let $z = f(x, y)$ be a function the graph of which is a neighborhood of p in bd K. Furthermore, for any $\phi \in [0, \pi]$, let $f_L(t) = f(t\cos\phi, t\sin\phi)$ be the restriction of f to the line L containing $(\cos\phi, \sin\phi)$ and the origin. Consider a value of R such that $\frac{1}{R}$ is strictly smaller than any of the two principal curvatures of bd K at p. Then $\frac{1}{R} < |f_L''(0)|$ for any line L. Since bd K is C^∞-class in a neighborhood of p, so is f in a neighborhood of $(0, 0)$. Thus, for some $\delta > 0$, $\frac{1}{R} < f_L''(t)$ for any $|t| \leq \delta$.

We choose δ satisfying this condition, and consider the part S, with points for the coordinates of which $\sqrt{x^2 + y^2} \leq \delta$ and $z > 0$, of the sphere of radius R that touches the plane $\{z = 1\}$ at p from the side containing the origin. Clearly, S is a closed spherical cap. Now, set C_R as the intersection of all closed half spaces that contain S and with their boundaries tangent to S. Then C_R is a 'cone with a rounded apex'. Note that C_R is convex, contains K, and that $(\operatorname{bd} C_R) \cap K = \{p\}$. Furthermore, the boundary of the translate $C_R(\varepsilon)$, with a sufficiently small vector $(0, 0, -\varepsilon)$ where $\varepsilon > 0$, intersects bd K in a simple smooth closed curve contained in the translate of the interior of the spherical cap S. Our first lemma describes the properties of the intersection $K_R(\varepsilon) = C_R(\varepsilon) \cap K$.

Lemma 7 *Let $\frac{1}{R}$ be smaller than any of the two principal curvatures of* bd K *at p. Then there are constants $\lambda_1, \lambda_2, \lambda_3 > 0$ depending only on R and K such that for every sufficiently small $\varepsilon > 0$ the following hold.*

(1) no point of (bd K) $\cap \mathbf{B}_{\lambda_1\sqrt{\varepsilon}}(p)$ *belongs to $K_R(\varepsilon)$.*
(2) (bd K) $\setminus \mathbf{B}_{\lambda_2\sqrt{\varepsilon}}(p) \subseteq K_R(\varepsilon)$.
(3) If D is a convex body, with center o' and satisfying $K_R(\varepsilon) \subseteq D \subseteq K$, then $|o'| \leq \lambda_3 \varepsilon^2$.

Proof First, observe that $K_R(\varepsilon)$ is convex, as it is the intersection of convex bodies.

Recall the two-variable function f from the definition of $K_R(\varepsilon)$. Like there, let $f|_L : \mathbb{R} \to \mathbb{R}$ denote its restriction $f|_L(t) = f(t\cos\phi, t\sin\phi)$, where $\phi \in [0, \pi]$, on a line L passing through the origin and $(\cos\phi, \sin\phi)$. Let h denote the one-variable function, defined on $[-R, R]$, the graph of which is a semicircle, of radius R, and with maximum $h(0) = 1 - \varepsilon$. By the conditions in Lemma 7, we have $0 > f|_L''(0) > h''(0)$. Hence, from the second-degree Taylor polynomials of $f|_L$ and h, we obtain that

$$\varepsilon - \lambda_1^\star t^2 < f_L(t) - h(t) < \varepsilon - \lambda_2^\star t^2$$

for some positive constants $\lambda_1^\star, \lambda_2^\star$. Thus, (1) and (2) clearly follow with $\lambda_1 = \frac{1}{\lambda_1^\star}$ and $\lambda_2 = \frac{1}{\lambda_2^\star}$.

Now we show (3). Let $o' = (x', y', z')$. Recall that

$$o' = \frac{\int_{q \in D} q \, \mathrm{d}V}{\int_{q \in D} 1 \, \mathrm{d}V}.$$

First, we estimate x'. Note that the part of K outside D can be covered by an axis-parallel brick of side-lengths $2\lambda_2\sqrt{\varepsilon}, 2\lambda_2\sqrt{\varepsilon}$ and $c\varepsilon > 0$ for some constant c independent of ε. Thus,

$$\left| \int_{q \in D} 1 \, \mathrm{d}V - \int_{q \in K} 1 \, \mathrm{d}V \right| \leq 4\lambda_2^2 c\varepsilon^2,$$

and

$$\left| \int_{q \in D} x \, \mathrm{d}V - \int_{q \in K} x \, \mathrm{d}V \right| \leq 4\lambda_2^3 c\varepsilon^{5/2},$$

from which $|x'| \leq \lambda_3' \varepsilon^2$ follows. In the same way, we may obtain similar bounds for y' and z', which readily yields the assertion.

We note that Lemma 7 can be applied for the degenerate case $R = \infty$ as well. The next lemma guaranties that the truncated body $K_R(\varepsilon)$ has the same numbers and types of static equilibrium points.

Lemma 8 *Let p be a stable point of K, or let p be an unstable point and $R < ||p||$. If R satisfies the conditions in Lemma 7, then there is an $\varepsilon > 0$ such that for every $t \in [0, \varepsilon]$ the following holds: $K_R(t)$ and $K = K_R(0)$ have the same number of stable/unstable and saddle points. Furthermore, the coordinates of these points are continuous functions of t.*

Proof Note that as the Euclidean distance function from a fixed point is C^∞-class at every point but the origin, all the partials of any order at any point of bd K change continuously when translating K. Hence, applying the Poincaré-Hopf Theorem [3] to a compact neighborhood of any equilibrium point shows that the numbers of the stable/unstable/saddle points of K do not change under a translation by a small vector, and their coordinates are continuous functions of the translation vector. Similarly, the gradient vector field changes continuously under a translation of K. Thus, o has a neighborhood U such that for any $u \in U$, the Morse-Smale complex of K is homeomorphic to that of $K + u$, or, in other words, the Morse-Smale complex of K with respect to u is homeomorphic to that with respect to o.

If t is sufficiently small, then the center o_t of $K_R(t)$ is contained in U. Hence, all the stable/unstable and saddle points of K but p change continuously as functions of t. Note that by (1) and (3) of Lemma 7, the stable/unstable point of K, with respect to o_t, that corresponds to p is contained in the part truncated by $C_R(t)$. Thus, this point does not belong to $K_R(t)$. On the other hand, by (2) of the same lemma, there is exactly one equilibrium point of $K_R(t)$ on the part belonging to $C_R(t)$.

We leave it to the reader to show that no plane, perpendicular to $[u, q]$ for some $u \in V$, supports $K_R(t)$ at a point $q \in (\mathrm{bd}\, K) \cap \mathrm{bd}\, C_R(t)$, and thus, there are no more equilibrium points of $K_R(t)$.

Now we show that there is a value of R for which the assertion in Lemma 5 holds. To do this, consider some $K_R(\varepsilon)$, where $\varepsilon > 0$ and $R > 0$ satisfy the conditions of Lemma 8. By this lemma, we may assume that $K_R(\varepsilon)$ has the same numbers of stable/unstable and saddle points as K does. Let o_R denote the center of $K_R(\varepsilon)$, and p_R be the critical point of $K_R(\varepsilon)$ corresponding to p. Consider a closed C^1-class curve $g \subset \mathrm{bd}\, K_R(\varepsilon)$, separating p_R from all the other critical points of $K_R(\varepsilon)$, which is disjoint from the truncated, spherical part, and is *not* tangent to any integral curve of bd K, with respect to o_R, that intersects g.

Now we show that even though bd $K_R(\varepsilon)$ is not C^1-class, we may still apply the smoothing algorithm described in Lemma 4. More specifically, we show that if we smooth $K_R(\varepsilon)$ using the function h_t described in the proof, then the Morse-Smale complex of the resulting body K' is homeomorphic to that of K. Let $g' \subset \mathrm{bd}\, K'$ be the curve corresponding to g. Observe that as the gradient vector field changes continuously as a function of t, for sufficiently small t g' is not tangent to any integral curve of K' intersecting it. Furthermore, any such integral curve ends at a critical point in the region inside g' and for small values of ε and t there is a unique critical point in this region, which we denote by p'. Thus, we may choose values of ε and t such that the Morse-Smale complex of K' is homeomorphic to that of K. By Remark 2, p' has a spherical neighborhood, and the radius of this sphere is arbitrarily close to R.

As a result of our consideration, we may assume that for *some* value of R, the examined critical point p has a spherical cap neighborhood in bd K of radius R. In the last lemma of the subsection, we show that this truncation can be carried out using a sphere of essentially any radius. To formulate it, recall that the integral curves connecting p to a saddle point of K are denoted by $\Gamma_1, \Gamma_2, \ldots, \Gamma_k = \Gamma_0$ in cyclic order around p.

Lemma 9 *Let K satisfy (*), and assume that p has a spherical cap neighborhood in bd K, of radius R. Let $0 < r < ||p||$ if p is an unstable point, and $r > ||p||$ if p is a stable point, and let $\delta > 0$ arbitrary. Then there is a convex body $K' \subseteq K$ satisfying (*) and the following.*

- *The Morse-Smale complex of K' is homeomorphic to that of K.*
- *Denoting the critical point of K' corresponding to p by p', p' has a spherical cap neighborhood in bd K', of radius arbitrarily close to r.*
- *Denoting the integral curve of K' corresponding to Γ_i by Γ_i' for every i, and by t_i' the unit tangent vector of Γ_i' at p', we have that $||t_i' - t_i|| < \delta$.*

Proof First, let $r < R$. Then we set $p' = p$. Let U be a (sufficiently small) neighborhood of o such that for every $u \in U$, the Morse-Smale complex of K with respect to u is homeomorphic to that with respect to o. By (3) of Lemma 7, there is an $\varepsilon > 0$ such that for any convex body K', satisfying $(K \setminus \mathbf{B}_\varepsilon(p)) \subseteq K' \subseteq K$, the center of K' is contained in U.

Clearly, we may replace the part of bd K in $\mathbf{B}_\varepsilon(p)$ with a surface of rotation S', with the line containing $[o, p]$ as its axis of symmetry, in such a way that:

- $p \in S' \subset K$ and $(\text{bd } K \setminus \mathbf{B}_\varepsilon(p)) \cup S'$ is the boundary of a convex body K',
- the modified body K' has a C^1-class boundary,
- a neighborhood of p in S' belongs to a sphere of radius r,
- there is no equilibrium point on S' but p, with respect to any point of U on the line containing $[o, p]$.

Note that the center of K' lies on the line containing $[o, p]$, and thus all the integral curves emanating from p in $\mathbf{B}_\varepsilon(p)$ are the meridians of S'. Let these curves be denoted by $\Gamma_1', \ldots, \Gamma_k' = \Gamma_0'$ in cyclic order, with t_i' denoting the unit tangent vector of Γ_i' at p. Thus, since the integral curves of K with respect to $u \in U$, connecting p and the saddle points of K are deformed continuously when modifying u, the assertion readily follows for sufficiently small U. To obtain a convex body with a C^∞-class boundary, we may finally apply Lemma 4.

If $r > R$, we may use a truncation by a sphere of radius r, like in the previous part of the subsection.

3.3 Proof of Lemma 6

Examples of geometric truncations generating combinatorially possible vertex splittings are shown in Figure 4. Note that in a vertex splitting, the edges around the vertex to be split are partitioned into two parts (one of which is possibly empty), in cyclic order, such that edges in the same part end up in the same split vertex.

First, we consider the case that vertex p to be split is a stable point of K. The truncation is illustrated in Figure 5.

Let the center of mass of K be the origin, and set $p = (0, 0, 1)$. According to the formulation of Lemma 5, we may choose the radius r' of the spherical neighborhood of p arbitrarily close to any given value $r > ||p|| = 1$. We choose the value of r later.
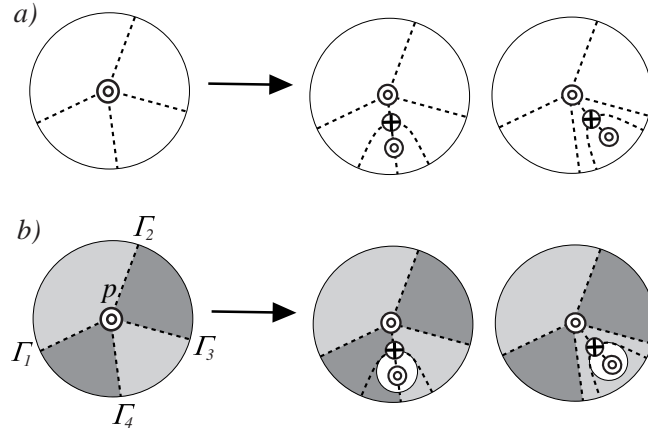
Fig. 4 Vertex splittings at vertex p. Here, p is a minimum point (of course, p could also be a maximum). a) Vertex splitting in the primal representation in class $\mathcal{Q}^{3\star}$ ($d(v) = 4$) b) Geometric realization with a truncation by a plane
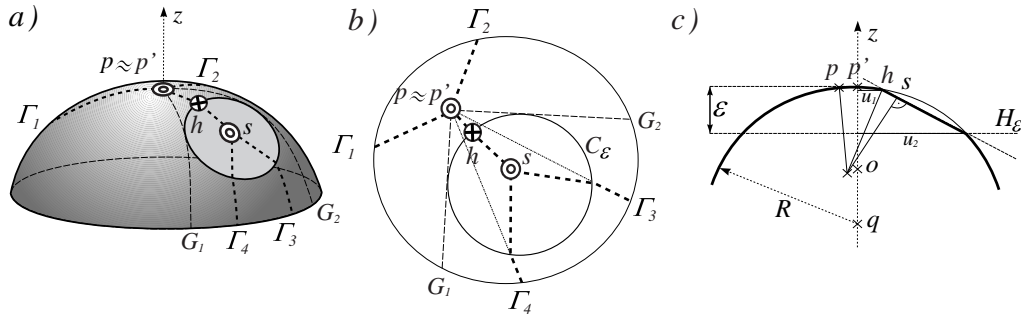
Fig. 5 Truncation with a plane

Let the integral curves of K, connecting p and the saddle points of K, in cyclic order around p, be Γ_i, where $i = 1, 2, \ldots, k$, and the unit tangent vector of Γ_i at p is t_i. Let R and q denote the radius and the center of the sphere, containing a spherical cap neighborhood of p. We denote this neighborhood by S. Then, according to Lemma 5, we may assume that R is arbitrarily close to any given number greater than $||p||$. Thus, the arc of any integral curve of K within S, including the Γ_is, are great circle arcs.

Let G_1 and G_2 be two open great circle arcs in S, starting at p, that are, in the interiors of the two regions, bounded by the Γ_is, that we want to split. These different regions are shaded in Figure 4 b). We may choose G_1 and G_2 in a way that they do not belong to the same great circle. We intend to truncate K near p with a plane in such a way that there is a new stable point on the plane, a new saddle point on its boundary, and the saddle point is connected to the stable point corresponding to p, to the stable point on the plane and to the two unstable points in the boundaries of the regions containing G_1 and G_2. To do this, we use a planar section that touches G_1 and G_2. To examine the properties of these sections, we first prove a technical lemma that we are going to use in the construction.

Lemma 10 *Let C be a circle in the plane $\mathbb{R}^2$ with the origin as its center and with radius 1. Let $p = (0, t)$ with $t > 0$. Let $q_1 = (u_1, v_1)$ and $q_2 = (u_2, v_2)$ be two points of C such that $v_1 > 0$.*

(1) If $[q_1, q_2]$ is perpendicular to $[p, q_1]$, then $\lim_{u_1 \to 0} \frac{u_2}{u_1} = \frac{2t}{1-t}$.

(2) If the angle of $[q_1, q_2]$ and $[p, q_1]$ is $\frac{\pi}{2} - cu_1$ for some constant c independent of u_1, then $\lim_{u_1 \to 0} \frac{u_2}{u_1} = \frac{2t}{1-t} + 2c$.

Proof We note that $u_2 = \frac{(1-t^2)u_1}{1 - 2\sqrt{1 - u_1^2 t + t^2}}$, from which (1) immediately follows. The second part can be proven with a similar elementary computation. Note that in the second case the angle between $[p, q_1]$ and the segment connecting p and its orthogonal projection on $[q_1, q_2]$ is cu_1.

Now, consider a spherical circle on S that touches G_1 and G_2, and let u_1 and u_2 denote, respectively, the distance of its closest and its farthest point from the z-axis. Let L denote the limit of u_2/u_1 as u_1 tends to zero. Note that this limit exists, is positive and does not depend on the radius of S, only on the angle of G_1 and G_2; this follows from the observation that spherical space 'locally' is Euclidean.

Now we choose the radius of the spherical neighborhood of p such that $2(R - 1) < L$ is satisfied. Thus, by (1) of Lemma 10, there is a sufficiently small circle C on S touching G_1 and G_2 such that the truncation of K by the plane containing C has a stable point, with respect to o, on the truncated, disk-shaped part. Furthermore, by (2) of the same Lemma, we may choose $0 < \tau < 1$ in a way that if C is sufficiently small, then the distance of this point from the boundary of C is at least τ times the radius of the circle.

Let H_ε denote the plane perpendicular to and intersecting $[o, p]$, at the distance ε from p. Let $\bar{K}_\varepsilon$ denote the truncation of K by this plane. Let U_ε be the set of the centers of all the convex bodies D satisfying $\bar{K}_{2\varepsilon} \subseteq D \subseteq K$. Clearly, we may choose a sufficiently small ε such that the Morse-Smale complex of K with respect to any point of U_ε is homeomorphic to that with respect to o. Furthermore, using (3) of Lemma 7, we may choose ε in a way that both the diameter of U_ε, and the diameter of the projection U_ε^S on S of U_ε from q is at most $c\varepsilon^2$ for some $c > 0$ independent of ε. Note that for small values of ε, these projections belong to S. Furthermore, for any fixed $\delta > 0$, we may also choose ε in a way that the intersection points, with the circle $K \cap H_\varepsilon$, of any integral curve connecting the projection of a point u from q on S and a saddle point of K with respect to u moves on an arc of angle not greater than δ, where u runs over U_ε. We denote these integral curves by $\Gamma_1^u, \Gamma_2^u, \ldots, \Gamma_k^u = \Gamma_0^u$.

Let C_ε be the circle that touches G_1, G_2 and H_ε on the side of H_ε not containing o, and K_ε be the truncation of K by the plane containing C_ε. Note that the radius of C_ε is at least $\bar{c}\sqrt{\varepsilon}$ for some positive constant $\bar{c}$. Thus, for sufficiently small ε, the following are satisfied.

– for any $u \in U_\varepsilon$, C_ε intersects exactly those curves from amongst the Γ_i^us that we want to intersect with the planar section.
– No such intersection point is on G_1 and G_2.

  − The orthogonal projection of U_ε on the plane of C_ε is contained in the interior
    of C_ε.
  − U_ε^S is contained in K_ε, and is disjoint from C_ε.

Clearly, under the conditions described in the previous paragraph, K_ε has
three equilibrium points in the closed half plane bounded by H_ε and containing
p: a stable point p' 'near' p (that is, in U_ε^S), another stable point s on the planar
disk bounded by C_ε, and a saddle point h on C_ε. This saddle point is connected to
both p' and s: the integral curve connecting it to p' is a great circle arc, and the
other one is a straight line segment. Furthermore, for every Γ_i on the truncated
side of $G_1 \cup G_2$, there is a (piecewise differentiable) integral curve of K_ε connecting
s to the corresponding saddle point of K_ε, and for every Γ_i on the other side of
$G_1 \cup G_2$, there is a similar curve ending at p'. This implies, by exclusion, that h is
connected to the two unstable points in the two chosen regions containing G_1 and
G_2.

Finally, observe that by replacing the truncating plane containing C_ε by a
ball of sufficiently large radius results in a homeomorphic Morse-Smale complex.
Furthermore, 'to smooth out' bd K_ε, we may replace C_ε by a sufficiently small
toroidal surface, which results in a convex body K' with a C^2-class boundary, such
that its Morse-Smale complex is homeomorphic to the one split in the required
way. We remark that $K_{2\varepsilon} \subseteq K'$, and thus, the center of K' is still contained in
U_ε. Finally, we may apply Lemma 4 to obtain a convex body with a C^∞-class
boundary, which finishes the proof for a stable point.

For an unstable point we may apply a similar consideration. In this case, instead
of a truncation with a ball of large radius, we expand the original ball with a
circular cone the axis of which contains the ball center q.

Remark 3 One may wonder whether we could have proven our statement using
only one local truncation by a plane. However, as we already indicated in the Intro-
duction, this appears to be impossible: The phenomenon described in Lemma 10
shows that to carry out an arbitrary splitting of an arbitrary (given) vertex we
need one additional free parameter and this is the radius of the truncating sphere.
In terms of local quantities, this implies that even in the special case when the
chosen equilibrium is an umbilical point (i.e. its vicinity is spherical), the required
splitting *cannot* be realized by a planar truncation unless the principal curvature
at this point is contained in a given interval determined by the directions of the
edges starting at this vertex. As a consequence, we need to adjust the principal
curvature *before* truncating with a plane. This step is achieved in Lemma 9.

4 Summary and related issues

The central idea of our paper is to associate vertex splittings with localized geo-
metric transformations. The latter are defined in such a way that we can control
all combinatorial possibilities. Next we show that vertex splittings arise in a spon-
taneous way in various geometric settings where they may or may not exhaust
the full combinatorial catalog. From this point of view, our construction creates a
framework to study these processes.

4.1 A road map for the generic bifurcations of one-parameter vector fields

If we consider generic, 1-parameter families of gradient vector fields on $\mathbb{S}^2$ then it is not true that every element of such a family is Morse-Smale. Rather, these families produce two types of singularities at which this property may fail: saddle-node bifurcations and saddle-saddle connections [4]. The former is a local bifurcation while the latter is a non-local bifurcation. A saddle-node bifurcation corresponds to a vertex splitting or a face contraction on the quasi-dual graph representation of the Morse-Smale complex, while a saddle-saddle connection corresponds to a transformation called *diagonal slide* [32]. Each gradient vector field can be uniquely associated with the quasi-dual graph representation of its Morse-Smale complex, so the evolution of one-parameter families can be studied on a metagraph $\mathcal{G}$ the vertices of which are graphs $Q^2 \in \mathcal{Q}^2$, representing the Morse-Smale complexes and the edges of $\mathcal{G}$ correspond to generic bifurcations in one-parameter families. Any such family will appear as a path on $\mathcal{G}$. Convex bodies associated with some selected graphs (selected vertices of $\mathcal{G}$) are illustrated in Figure 6/a3. A small portion of $\mathcal{G}$ is illustrated in Figure 6/a1. Solid edges represent saddle-node bifurcations, dashed edges represent saddle-saddle connections, Figure 6/a2 shows the latter inside the primary equilibrium class $\{S, U\} = \{2, 3\}$. Theorem 1 states that all vertices of $\mathcal{G}$ can be represented with suitably chosen, smooth convex bodies. We did not prove the existence of convex bodies carrying gradient fields which exhibit the codimension 1 bifurcations, corresponding to the edges of $\mathcal{G}$. Nevertheless, as we point out below, our geometric construction suggests that solid edges (saddle-nodes) exist on convex bodies. Consider two secondary classes corresponding to two vertices of $\mathcal{G}$ and assume that they are in adjacent primary classes, i.e. either the number of stable points or the number of unstable points differs by one (but not both). Such pairs neighbour secondary classes can be observed in Figure 6/a1, for example (b, c), (c, e), (c, f). It follows from our geometrical construction (Lemma 3) that if this pair of vertices of $\mathcal{G}$ are connected by an edge (e.g. (b, c), (c, e)) then there is a one-parameter family $K(\lambda)$ of convex bodies between those two secondary classes that except for one arbitrary short interval $\lambda \in (\lambda^\star - \epsilon, \lambda^\star + \epsilon)$, all convex bodies $K(\lambda)$ are generic. Based on this we formulate

Conjecture 1 For any generic, one-parameter family $\mathbf{v}(\lambda)$ of gradient vector fields on $\mathbb{S}^2$ exhibiting a codimension 1 saddle-node bifurcation for one single isolated parameter value $\lambda = \lambda^\star$ there exists a one-parameter family $K(\lambda)$ of (not necessarily smooth) convex bodies with gradient fields $\nabla r_{K(\lambda)}$ such that the latter is topologically equivalent to $\mathbf{v}(\lambda)$ for every value of λ.

Theorem 1, together with Conjecture 1 state that the *oriented* subgraph $\mathcal{G}_v \subset \mathcal{G}$ (illustrated in Figure 6/b1) containing only vertex splittings, exists among gradient fields associated with convex bodies. Combinatorial expansion sequences (2) associated with an n-vertex graph $Q_n \in \mathcal{Q}_n$ appear on this oriented metagraph as an oriented path of length $n - 2$, starting at the root (P_2). Observe that in the kth step a vertex in the box-diagonal $S + U = k$ is selected. Two such sequences are illustrated in Figure 6/b2. As pointed out above, beyond saddle-nodes, one-parameter gradient fields also undergo generic, codimension 1 saddle-saddle bifurcations which are non-local, however, it is not known whether there exists a geometric correspondence for this combinatorial connection inside the primary

equilibrium classes. Although our current geometric argument does not provide any direct hint for their existence on convex bodies, nevertheless we formulate

Conjecture 2 For any generic, one-parameter family $\mathbf{v}(\lambda)$ of gradient vector fields on $\mathbb{S}^2$ exhibiting any codimension 1 bifurcation for one single isolated parameter value $\lambda = \lambda^\star$ there exists a one-parameter family $K(\lambda)$ of (not necessarily smooth) convex bodies with gradient fields $\nabla r_{K(\lambda)}$ such that the latter is topologically equivalent to $\mathbf{v}(\lambda)$ for every value of λ.

stating that all edges of the metagraph $\mathcal{G}$ can be realized among convex bodies. Beyond theoretical interest, these metagraphs admit the study of interesting physical phenomena some of which we briefly discuss below.

4.2 Inhomogeneous bodies

Our first example is inhomogeneous bodies. So far, throughout the paper we assumed convexity and material homogeneity. Relaxing the latter constraint is equivalent to keep the convex surface bd K as the boundary of the body but let the mass be concentrated at the center of gravity C. As the location of C is varied in time as a curve $\mathbf{r}_C(t)$, it generates a one-parameter family of gradient vector fields on bd K. A classical result in catastrophe theory states that the number of critical points of the gradient changes if and only if $\mathbf{r}_C(t)$ transversely passes through one of the two caustics of the body [33]. Caustics (also known as focal surfaces) are the two surfaces formed by the curvature centers corresponding to the principal curvatures of bd K. Figure 7 a)-c) shows the two caustics of an ellipsoid, a) corresponding to curvature minimum, b) corresponding to curvature maximum, c) intersection (superposition) of both caustics. When $\mathbf{r}_C(t)$ transversely crosses the caustic defined by the minimal principal curvature, a saddle and an unstable point meet at a saddle-node; when $\mathbf{r}_C(t)$ transversely crosses the other caustic, a saddle and a stable point collide. Every saddle-node bifurcation corresponds to a vertex splitting (or face contraction, depending on the direction) on the quasi-dual Morse-Smale graph, so at each such event the corresponding path on $\mathcal{G}$ will move from one box-diagonal $S + U = k$ to one of its neighbor diagonals. Figure 7 d) shows the different Morse-Smale graphs in the different domains determined by the intersections of the two caustics. It is easy to see that if C is located far enough from the center of gravity of the homogeneous body then the corresponding Morse-Smale complex is represented by the path graph P_2.

4.3 Collisional abrasion: chipping of rocks

Our second example is pebble abrasion via collisions. This process is most often described by averaged geometric PDEs, the most general such model is given by Bloore [8] as

$$v = 1 + 2bH + cK \tag{5}$$
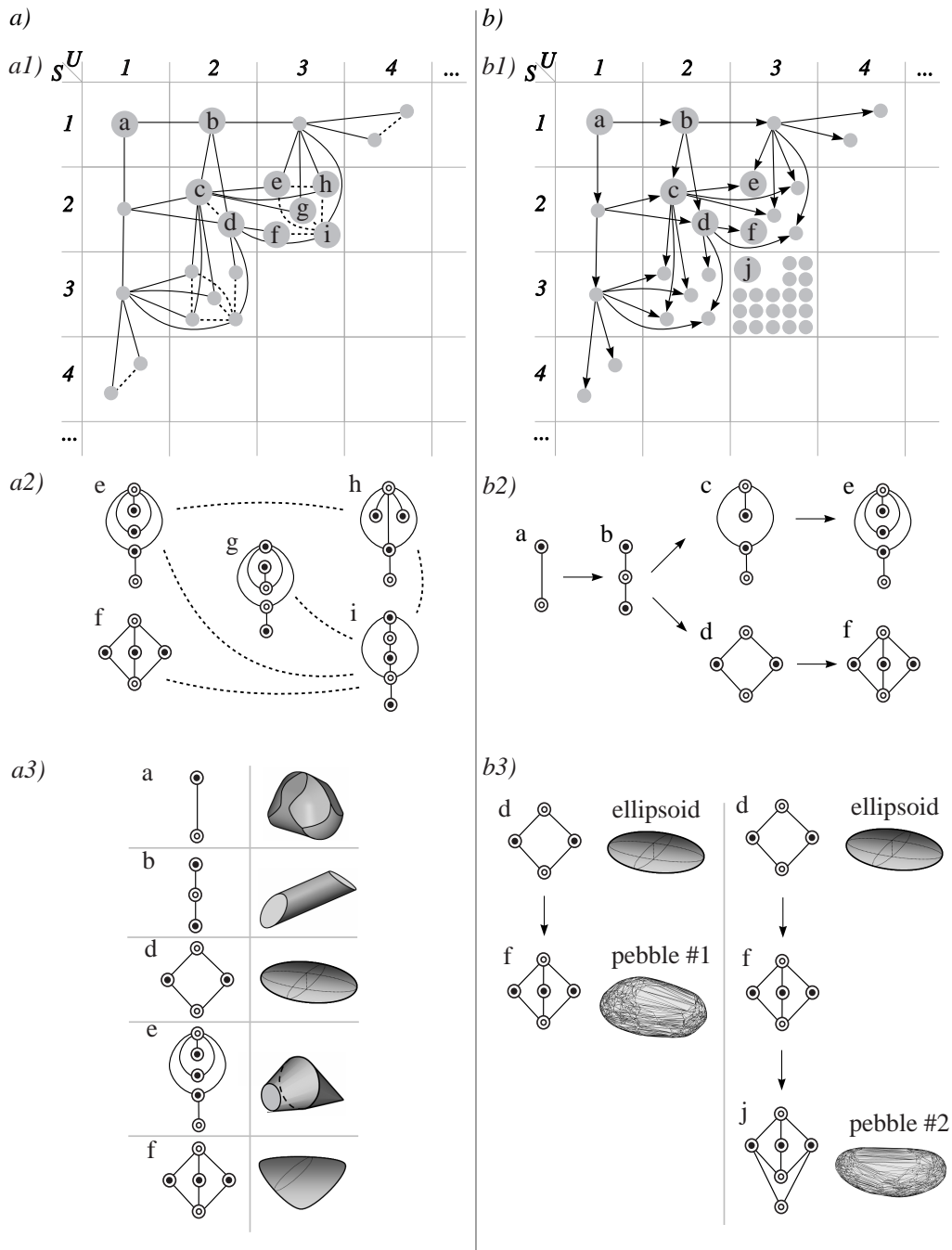
Fig. 6 a1) Metagraph $\mathcal{G}$ corresponding to generic bifurcations in one-parameter families of vector fields on the sphere a2) Saddle-saddle connections inside the primary equilibrium class $\{S, U\} = \{2, 3\}$ a3) Examples for convex bodies with some selected graphs b1) Oriented subgraph $\mathcal{G}_v \subset \mathcal{G}$ corresponding to vertex splittings b2) Two selected combinatorial expansion sequences b3) Morse-Smale complexes associated with real pebbles, derived with expansion sequences from the ellipsoid

where v is the attrition speed along the inward surface normal, H, K are the Mean and Gaussian curvatures, b, c are constants. Solutions of these PDEs correspond to (inward propagating) wave fronts. The actual physical process is somewhat different: it is based on discrete collisions where small amounts of material are being removed in a strongly localized area. Simple but natural interpretations of the discrete, physical abrasion process are *chipping algorithms* [19],[35] and [31] where in each step a small amount of material is chipped off at point p by intersecting the body with a plane resulting as a small parallel translation of the tangent at p. We call such an operation a *chipping event* and their sequence a *chipping sequence.*

In Section 3 we showed that any vertex splitting can be achieved by a suitably chosen convexity-preserving local truncation. It is not very difficult to show a related, though converse statement: any *sufficiently small* chipping event will either leave the Morse-Smale complex invariant or result in one or two consecutive vertex splittings. If we regard the material abraded in a chipping event as a random variable χ with very small, but finite expected value $E(\chi)$ and very small variance (as it is often done in chipping algorithms) then we expect that for some time intervals chipping events will be sufficiently small to form finite chipping sequences the *subsequences* of which are geometric expansion sequences of type (3).

Chipping sequences do not represent a rigorous, algorithmic discretization of the PDEs, rather, they can be regarded as an alternative, discrete approximation of the physical process. As it was pointed out in [17] and [18], pebble surfaces display equilibria on two, well-separated scales. While the PDE description accounts for the evolution of global equilibria, local equilibria, corresponding to the fine structure of the surface are only captured by the chipping model. Figure 8 shows the high-accuracy scan of a real pebble with equilibria and the primal representation of the Morse-Smale complex. We can observe flocks of local equilibria accumulated around global equilibrium points. In fact, one motivation behind chipping algorithms is to better understand the interplay between the two scales. Chipping models appear to be successful in explaining laboratory experiments (cf. [31] and [35]) as well as geological field observations [35]. The connection between chipping models and our geometric expansion algorithms suggests that the number of *local* equilibrium points may increase in abrasion processes for finite time intervals. Whether and how this process interacts with the evolution of *global* equilibria is an open question not addressed in the current paper.

Figure 6/b3 illustrates two, rather short geometrical expansion sequences leading to Morse-Smale complexes associated with real pebbles. While the abrasion of these pebbles was not monitored, given their simple Morse-Smale complex and nearly-ellipsoidal shape it is realistic to assume that these geometric expansion sequences are subsequences of the actual physical abrasion process (modeled by chipping sequences) which produced these shapes. Needless to say, many more experiments are needed to verify this theory.

4.4 Concluding remarks

In this paper we showed that Morse-Smale functions $\mathcal{M}_C$ associated with convex bodies exhaust all combinatorial possibilities, i.e., to any two-colored quadrangu-

lation $\bar{Q}^2 \in \mathcal{Q}^2$ on $\mathbb{S}^2$ there exists a convex body $\bar{K}$ such that $\bar{Q}$ is the quasi-dual representation of the Morse-Smale complex associated with $\bar{K}$. We proved our claim by showing that to each possible combinatorial expansion sequence Q_i^2 generated by vertex splittings, there exists a coupled geometric expansion sequence K_i such that Q_i^2 is the quasi-dual representation of the Morse-Smale complex associated with K_i. Geometric expansion sequences were created by local, convexity preserving truncations of the convex body. Beyond proving the existence of all combinatorially possible convex shapes, we also generalized the classification scheme of [36]. We also showed that geometric expansion sequences appear to be part of the natural geometrical description of collisional abrasion.

5 Acknowledgement

References

1. E.M. Andreev, Convex polyhedra in Lobachevsky spaces, Math. Sb. (N.S.) 81(123) (1970), 445-478.
2. Archdeacon, D., Hutchinson, J., Nakamoto, A., Negami, S. and Ota, K., Chromatic numbers of quadrangulations on closed surfaces, J. Graph Theory 37 (2001), 100-114.
3. Arnold, V.I., Ordinary differential equations, 10th printing, MIT Press, Cambridge, 1998.
4. Arnold, V.I. (Ed.), Dynamical Systems V: Bifurcation Theory and Catastrophe Theory, Springer-Verlag, Berlin, 1994.
5. Bagatelj, V., An inductive definition of the class of 3-connected quadrangulations of the plane, Discrete Math. **78** (1989), 45-53.
6. Bauer, U., Lange, C. and Wardetzky, M., Optimal topological simplification of discrete functions on surfaces, Discrete Comput. Geom. 47 (2012), 347-377.
7. Bonnesen, T., Fenchel, W., Theory of Convex Bodies, Moscow, Idaho: L. Boron, C. Christenson and B. Smith, BCS Associates, 1987.
8. Bloore, F.J., The Shape of Pebbles, Math. Geol. 9 (1977) 113-122.
9. Bremer, P.T., Edelsbrunner, H., Hamann, B. and Pascucci, V., A multi-resolution data structure for two-dimensional Morse-Smale functions, Proceeding VIS '03 (2003), 139-146.
10. Brinkmann, G., Greenberg, S., Greenhill, C., McKay, B.D., Thomas, R. and Wollan, P., Generation of simple quadrangulations of the sphere, Discrete Math. 305 (2005), 33-54.
11. Brinkmann, G. and McKay, B.D., Fast generation of planar graphs, MATCH Commun. Math. Comput. Chem 58 (2007), 323-357.
12. Conway, J.H. and Guy, R., Stability of polyhedra, SIAM Rev. 11 (1969), 78-82.
13. Dawson, R., Monostatic Simplexes, Amer. Math. Monthly 92 (1985), 541-546.F
14. Dawson, R. and Finbow, W., What shape is a loaded die?, Math. Intelligencer 22 (1999), 32-37.
15. Dey, T.K., Li, K., Luo, C., Ranjan, P., Safa, I. and Wang, Y., Persistent Heat Signature for Pose-oblivious Matching of Incomplete Models, Computer Graphics Forum 29 (2010), 1545-1554.
16. Diestel, R., Graph Theory, 3rd edition, Springer-Verlag, Heidelberg, 2005.

17. Domokos G., Lángi Z. and Szabó, T., On the equilibria of finely discretized curves and surfaces, Monatsh. Math. 168 (2012) 321-345.
18. Domokos G., Sipos A.Á. and Szabó, T., The mechanics of rocking stones: equilibria on separated scales, Math. Geosci. 44 (2012), 71-89.
19. Domokos G., Sipos A.Á. and Várkonyi P. Continuous and discrete models for abrasion processes, Per. Pol. Arch. 40 (2009) 3-8.
20. Dong, S., Bremer, P.-T., Garland, M., Pascucci, V. and Hart, J.C., Spectral surface quadrangulation, ACM T. Graphic 25 (2006), 1057-1066.
21. Edelsbrunner, H., Harer, J. and Zomorodian, A., Hierarchical Morse-Smale complexes for piecewise linear 2-manifolds, Discrete Comput. Geom. 30 (2003), 87-107.
22. Evans, L., Partial differential equations, Graduate Texts in Mathematics 19, American Mathematical Society, Providence RI, 1998.
23. Fusy, E., Counting unrooted maps using tree-decomposition, Seminaire Lotharingien de Combinatoire 54A (2007), Article B54Al
24. Ghomi, M., The problem of optimal smoothing for convex functions, Proc. Amer. Math. Soc. 130 (2002), 2255-2259.
25. Gross, J. T. and Yellen, J., Graph Theory and Its Applications, 2nd ed., Boca Raton, FL: CRC Press, 2006.
26. Gyulassy, A., Natarajan, V., Pascucci and V., Hamann, B., Efficient computation of Morse-Smale complexes for three-dimensional scalar functions, IEEE Trans. Vis. Comput. Graph. 13 (2007), 14401447.
27. Heath, T. I. (Ed.), The Works of Archimedes, Cambridge University Press, 1897.
28. Heppes, A., A double-tipping tetrahedron, SIAM Rev. 9 (1967), 599-600.
29. Hirsch, M., Differential topology, Graduate Texts in Mathematics 33, Springer-Verlag, New York-Heidelberg, 1976.
30. Kápolnai, R. and Domokos, G., Inductive generation of convex bodies, in: The 7th Hungarian-Japanese Symposium on Discrete Mathematics and Its Applications, 2011, pp. 170-178.
31. Krapivsky, P.L. and Redner S., Smoothing a rock by chipping, Phys. Rev. E 9 (2007), 75(3 Pt 1):031119.
32. Negami, S. and Nakamoto, A., Diagonal transformations of graphs on closed surfaces, Sci. Rep. Yokohama Nat. Univ., Sec. I 40 (1993), 71-97.
33. Poston, T. and Stewart, J., Catastrophe theory and its applications, Pitman, London, 1978.
34. R.K.W. Roeder, J.H. Hubbard and W.D. Dunbar, Andreev's theorem on hyperbolic polyhedra. Ann. Inst. Fourier (Grenoble), 57(3) (2007), 825-882.
35. Sipos A.Á., Domokos G., Wilson A. and Hovius N. A Discrete Random Model Describing Bedrock Erosion, Math. Geosci. 43 (2011) 583-591.
36. Várkonyi, P.L. and Domokos, G., Static equilibria of rigid bodies: dice, pebbles and the Poincaré-Hopf Theorem, J. Nonlinear Sci. 16 (2006), 255-281.
37. Zamfirescu, T., How do convex bodies sit?, Mathematica 42 (1995), 179-181.
38. Zomorodian, A., Topology for computing, Cambridge University Press, 2005.
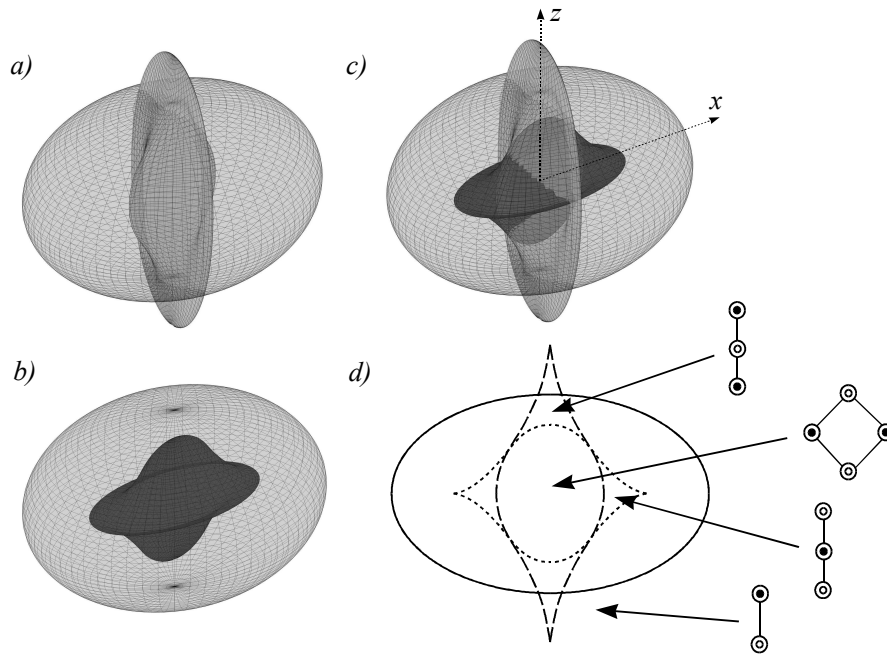
Fig. 7 Caustics of an ellipsoid. a) Caustic defined by the minimal principal curvature b) Caustic defined by the maximal principal curvature c) Superposition of the two caustics d) Quasi-dual Morse-Smale graphs (in class $\mathcal{Q}$) in the different domains, shown on the plane section through axes x and z

a)

b)
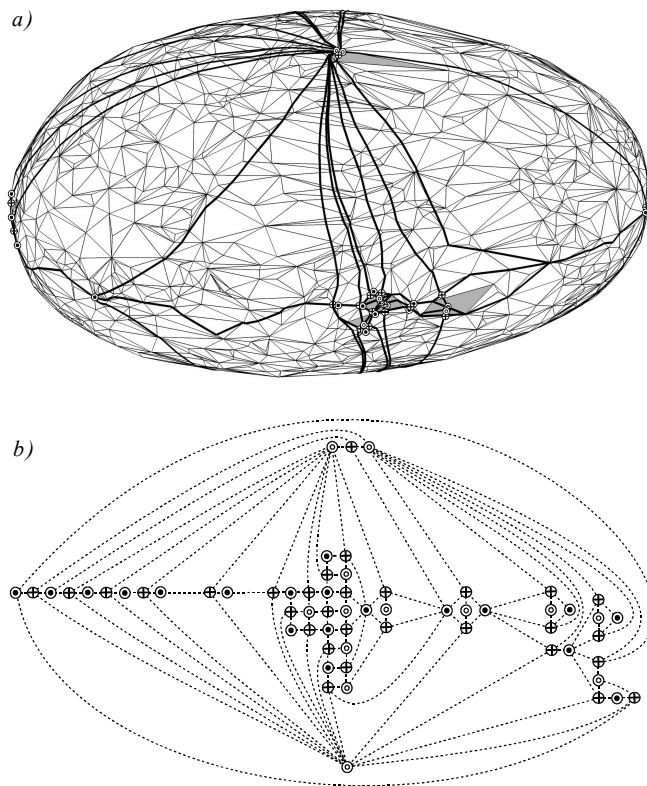
Fig. 8 The Morse-Smale complex of a real pebble: primal Morse-Smale graph in class $\mathcal{Q}^{3\star}$ a) drawn on the pebble's surface b) drawn on the plane